Poster #W91A

A Mechanism Denial Study on the Madden-Julian Oscillation

Daehyun Kim[1] (dkim@ldeo.columbia.edu), Adam H. Sobel[1,2,3], and In-Sik Kang[4]

[1]Lamont-Doherty Earth Observatory of Columbia University, Palisades, NY, [2]Department of Applied Physics and Applied Mathematics, Columbia University, New York, NY,
[3]Department of Earth and Environmental Sciences, Columbia University, New York, NY, [4] Seoul National University, Seoul, South Korea

1. Motivation

Although there are several known ways to improve the Madden-Julian osciilation (MJO) in model simulations, there have been limited attempts to understand the improvement of a general circulation model (GCM) simulation in the frameworks of the existing theories. When we change a convection scheme so that the simulated MJO strengthens, what is the macroscopic mechanism by which that simulated MJO is initiated and maintained?

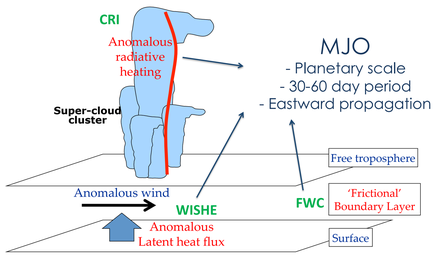

Figure 1. Schematic diagram of macroscopic mechanism of the MJO

6. Moisture anomaly associated with MJO

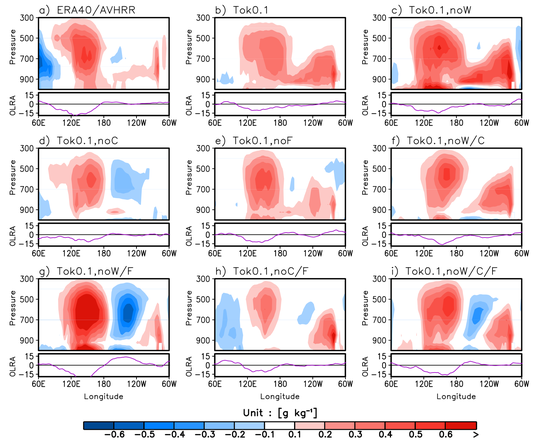

FIG4. MJO life-cycle composite of 20-100 day bandpass filtered, 10°S-10°N averaged specific humidity anomaly (upper panel), and filtered, 10°S-10°N averaged OLR anomaly (lower panel) at different phases in which the convective anomaly is located near the Maritime continent.

7. Role of WISHE

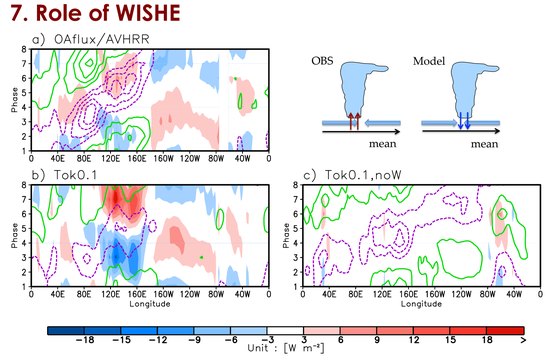

FIG 5. Phase–longitude diagram of OLR [contour plotted every 5 W m^{-2}, positive (green) and negative (purple)] and surface latent heat flux (W m^{-2}, shaded). Phases are from the MJO life cycle composite with values averaged between 10°S and 10°N. a) OAflux/AVHRR, b) Tok0.1, and c) Tok0.1,noW.

the negative impact of WISHE results from an unrealistic simulation of the phase relationship between precipitation and surface winds in the control simulation, with the surface easterly anomalies being shifted too far west (thus too much in phase with enhanced convection).

2. Experimental Design

Name	Variable	Treatment
Control (Tok0.1)	Everything is interactive	
noWISHE = noW (Wind-Induced Surface Heat Exchange)	Surface evaporation	Daily climatology prescribed (from control)
noCRI = noC (Cloud-Radiation Interaction)	Net radiative heating rate	
noFWC = noF (Frictional wave-CISK)	Surface wind stress (20S-20N only)	

3. MJO mechanism denial experiments

	Tok0.1	no W	no C	no F	no W/C	no W/F	no C/F	no W/C/F
WISHE	on	off	on	on	off	off	on	off
CRI	on	on	off	on	off	on	off	off
FWC	on	on	on	off	on	off	off	off

***SNUGCM, AMIP, period: 1979-2005**

5. MJO metrics derived from CEOF analysis

	OBS	Tok0.1	no W	no C	no F	no W/C	no W/F	no C/F	no W/C/F
%VAR	43.8	26.1	37.5	26.3	24.0	29.0	35.0	25.6	29.7
Coh^2	0.79	0.67	0.73	0.49	0.52	0.42	0.69	0.48	0.40
%30-80d	58.1	42.7	45.6	30.6	34.8	32.4	42.6	30.7	29.3

*** %VAR: percentage variance explained by the first leading pair of CEOF**
*** Coh2: coherence squared between two PCs of leading pair of CEOF within 30-80 day period**
*** %30-80d: percentage of power residing within 30-80 day period to total in power spectrum of 1st unfiltered PC**

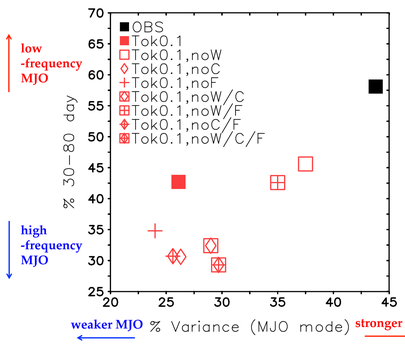

FIG 3. Scatterplot of the %VAR and %30-80d metric for MJO mode. Closed squares show observations (black), and Tok0.1 (red). Open square, open diamond, and cross symbols represent simulations without WISHE, CRI, and FWC, respectively. Combinations of open and cross symbols indicate double or triple mechanism denial experiments.

CRI and WISHE are both found to be important to the simulated MJO amplitude and propagation speed, while FWC has weaker and less systematic effects. The MJO is weakened when CRI is turned off, but strengthened when WISHE is turned off, indicating that CRI amplifies the MJO in the control simulation while WISHE weakens it.

8. Role of cloud-radiation interaction

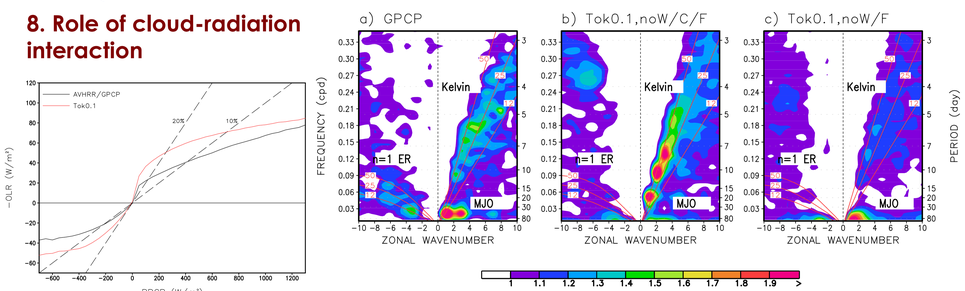

FIG 6 (left). Negative OLR anomaly (W m^{-2}) composited based on precipitation (W m^{-2}). The unit of precipitation in this plot is converted to condensational heating rate. Points over the warm pool region (40-180°E, 20°S-20°N) are used in calculations. Solid lines represent observations (black) and Tok0.1 (red). The two black dashed lines show 10% and 20% of precipitation, respectively.

FIG 7 (right). Space–time spectrum of the 15°N–15°S symmetric component of precipitation divided its estimated background spectrum. a) GPCP, b) Tok0.1,noW/C/F, and c) Tok0.1,noW/F. Superimposed are the dispersion curves of the odd meridional mode numbered equatorial waves for the equivalent depths of 12, 25, and 50m.

The positive influence of CRI in the model is consistent with a strong simulated relationship between daily grid-point column-integrated radiative and convective heating; the mean ratio of the latter to the former exceeds 0.2 for rain rates less than 14 mm d^{-1}. CRI is also shown to suppress an excessive excitation of the convectively coupled Kelvin wave so that the amplitude and frequency of the MJO is maintained.

4. Combined EOF

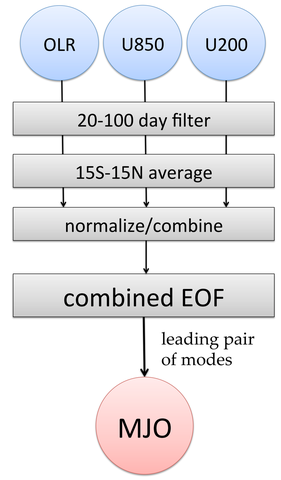

The MJO is defined here as the leading mode of coherent variability between anomalies in OLR and those in upper and lower tropospheric zonal wind.

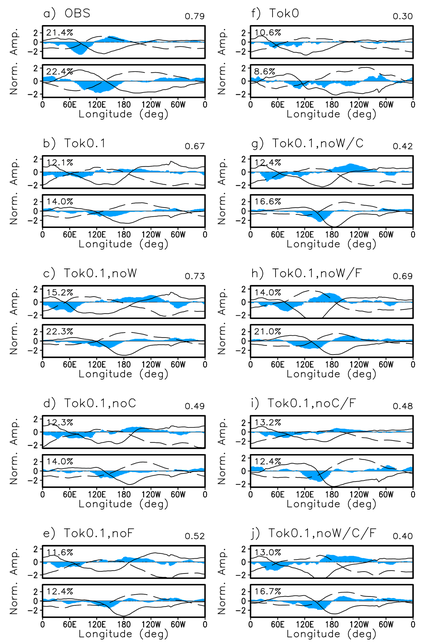

FIG 1. First two CEOF modes of 20–100-day 15°S–15°N averaged 850-hPa and 200-hPa zonal wind and OLR. The total variance explained by each mode is shown in the upper left of each panel. The mean coherence squared between principal components of two modes within a 30–80-day period is given above the upper panel.

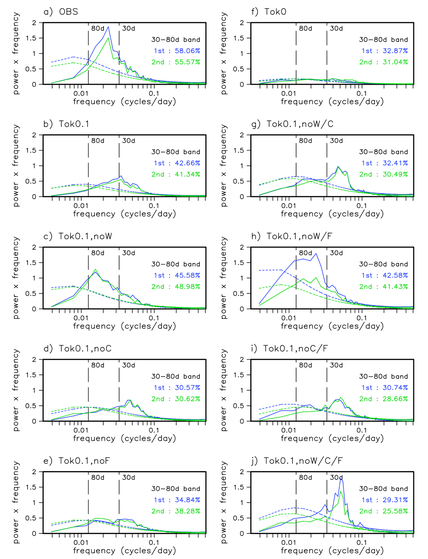

FIG 2. The power spectrum of the unfiltered PC derived by projecting the CEOFs onto unfiltered data (seasonal cycle removed): first mode (blue) and second mode (green). Dashed lines show the 99% confidence limit for a red noise spectrum.

9. Role of Frictional wave-CISK

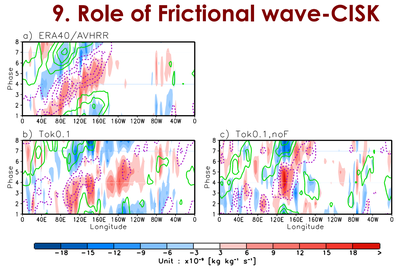

FIG. 8. As in Figure 5 but for 925-hPa moisture convergence (kg kg-1 s-1). a) ERA40/AVHRR, b) Tok0.1, and c) Tok0.1,noF.